RevMexAA (Serie de Conferencias), **31**, 61–70 (2007)

TURBULENCE PROFILES FROM THE SCINTILLATION OF STARS, PLANETS, AND MOON

Andrei Tokovinin[1]

RESUMEN

La turbulencia atmosférica puede ser caracterizada por el centelleo de las fuentes astronómicas. Se presenta una breve revisión de la física del centelleo débil y fuerte. El Sensor de Centelleo Multi-Apertura, MASS, utiliza las propiedades espaciales del centelleo producido por una estrella para reconstruir perfiles de turbulencia de baja resolución. Se presenta una descripción del instrumento combinado MASS-DIMM y se evalúa la precisión de este método. Se describe el experimento de remplazar la estrella por un planeta, ya que en ese caso se puede sensar la turbulencia a unos cuantos cientos de metros sobre el sitio. Sin embargo, de mayor importacia es medir la turbulencia en la vecindad inmediata de un telescopio o un monitor del sitio. En este caso, un medidor de centelleo lunar es el método a elegir. Un medidor de centelleo lunar, LuSci, está siendo desarrollado por el Observatorio Inter-Americano de Cerro Tololo (CTIO). Se presenta el nuevo método para interpretar sus datos y los resultados de las primeras pruebas.

ABSTRACT

Atmospheric turbulence can be characterized by the scintillation of astronomical sources. The physics of weak and strong scintillation is briefly recalled. The Multi-Aperture Scintillation Sensor, MASS, uses spatial properties of the scintillation produced by single stars to reconstruct low-resolution turbulence profiles. A description of the combined MASS-DIMM instrument is given and the accuracy of this method is evaluated. By replacing a single star with a planet, we can sense turbulence at few hundred meters above the site, and such an experiment is described. However, of greater importance is to measure the turbulence in the immediate vicinity of a telescope or site monitor. Here, lunar scintillation is the method of choice. A simple lunar scintillometer, LuSci, is under development at CTIO. A new method to interpred its data and the results of first tests are presented.

Key Words: **ATMOSPHERIC EFFECTS — SITE TESTING — TURBULENCE**

1. INTRODUCTION

Twinkling of the stars —scintillation— is the most obvious manifestation of atmospheric optical turbulence which causes "seeing". Can we use this phenomenon for a quantitative measurement of seeing? A scintillation-based device, *scintillometer*, is insensitive to the angular pointing and typically has small apertures, thus favoring its application for site-testing in the field.

One of the first attempts to extract turbulence profiles from scintillation has been undertaken by Ochs et al. (1976). It has been established earlier that the strength of scintillation measured through a 10-cm aperture is closely related to the isoplanatic angle. Krause-Polstorf et al. (1993) compared isoplanatic angles measured by this method with those derived from the scintillometer of Ochs et al.

Scintillation coming from different layers can be disentangled by using a double star. This method, called *Scidar*, has been developed by J. Vernin et al. and appears to be the best direct optical technique of turbulence profiling available to date. Originally, Scidar was not sensitive to the near-ground turbulence because it does not produce any scintillation. However, a modification of this method proposed by Fuchs et al. (1998) and called *Generalized Scidar* is free from this problem and can measure complete turbulent path, from the telescope to the top of the atmosphere.

The Scidar method has two problems: it requires suitably bright double stars and a large ($\geq$ 1m) aperture. A need for a simple single-star turbulence profiler has driven us to develop a *Multi-Aperture Scintillation sensor*, MASS, described below in § 3. Recently, a new instrument, *Single-Star Scidar*, has been proposed by Habib et al. (2006). It records scintillation of single stars and separates contributions of different turbulent layers by spatio-temporal analysis.

[1] Cerro Tololo Inter-American Observatory, Casilla 603, La Serena, Chile (atokovinin@ctio.noao.edu).

Planets, unlike stars, do not scintillate. Their angular diameter effectively averages scintillation produced by high turbulent layers. However, some weak scintillation originating mostly in low layers does remain. It can be measured and used to probe low-altitude turbulence. Such experiment is described in § 5. Pushing this idea to the extreme, we can even measure the scintillation of the Sun or Moon. In this case, the amplitude of the scintillation is very small, and it probes air in the immediate vicinity (few tens of meters) from the ground. The idea to use solar scintillation for turbulence measurements has been developed by Beckers (2001) and implemented in the instrument called *Shabar*. It proved to be decisive in the modern campaign of day-time site testing (Socas-Navarro et al. 2005). We discuss the use of lunar scintillation in § 6.

2. PHYSICS OF SCINTILLATION

Corrugations of the wave-front produced by the turbulence can be thought of as weak lenses. When such a lens is positive, it focuses the light and the intensity at the ground increases, while a negative lens does the opposite. This simple geometric-optics view is correct for large-scale perturbations (Figure 1). For perturbations comparable to or smaller than the *Fresnel radius* $\sqrt{\lambda z}$ (λ is the wavelength, z is the propagation distance) the interference of light becomes significant, hence such "lenses" act rather as diffraction gratings. Consequently, scintillation at small spatial scales $r < \sqrt{\lambda z}$ is wavelength-dependent, but at larger scales it is achromatic.

The theory of light propagation through weak turbulence is well developed (Tatarskii 1961; Roddier 1981). It predicts that the spatial spectrum of the light-wave amplitude χ passing through a weak phase screen and propagating over a distance z is

$$\Phi_\chi(\mathbf{f}) = 0.0229 r_0^{-5/3} |\mathbf{f}|^{-11/3} \sin^2(\pi \lambda z |\mathbf{f}|^2) \quad . \quad (1)$$

The spectrum of intensity fluctuations (scintillation) is $\Phi_I = 4\Phi_\chi$. Here, $\mathbf{f}$ is the 2-dimensional spatial frequency (in m^{-1}) and $r_0^{-5/3} = 0.423 (2\pi/\lambda)^2 C_n^2 \mathrm{d}z$ is the Fried parameter of a turbulent layer with refractive-index fluctuations C_n^2 and thickness dz.

An example of the spectrum (1) is shown in Figure 2. The first maximum is at a frequency $f \approx (\lambda z)^{-1/2}$, i.e. inverse of the Fresnel radius. At lower spatial frequencies, in the geometric-optics regime, we can replace the sine by its argument, so the spectrum becomes proportional to $f^{-11/3+4} = f^{1/3}$. This is the spectrum of the wave-front curvature, which is nearly white for Kolmogorov turbulence.

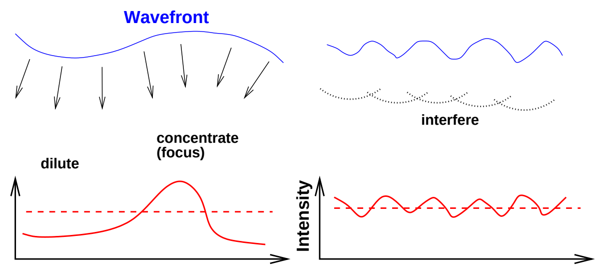

Fig. 1. Qualitative explanation of the scintillation from the geometric-optics (left) and wave optics (right) perspectives.

The curvature is achromatic, $r_0^{-5/3} \propto \lambda^{-2}$. Interestingly, atmospheric errors in photometry and differential astrometry are also proportional to the large-scale wave-front curvature, and hence can be directly inferred from scintillation (Kenyon et al. 2006).

An aperture of diameter D acts as a spatial filter, admitting only fluctuations with $|\mathbf{f}| < D^{-1}$. To calculate the total scintillation power, we have to multiply the spectrum (1) with a suitable aperture filter, integrate it, and multiply by 4. The result will be a *scintillation index* s_A^2, defined as

$$s_A^2 = \frac{\langle \Delta I_A^2 \rangle}{\langle I_A \rangle^2} \quad , \quad (2)$$

where I_A is the instantaneous light intensity received through some aperture A, ΔI_A is its fluctuation. The definition is equivalent to the variance of $\log I$ for weak scintillation. Although the turbulence theory usually operates with the variances of the logarithm, in practice formula (2) must be used because it permits correct treatment of photon counts rather than intensities (Tokovinin et al. 2003).

With apertures of different size, we can distinguish the altitude where the scintillation was produced (e.g., Kornilov & Tokovinin 2001). An even better method is to measure the *differential scintillation index* s_{AB}^2 between two apertures A and B,

$$s_{AB}^2 = \left\langle \left(\frac{\Delta I_A}{\langle I_A \rangle} - \frac{\Delta I_B}{\langle I_B \rangle} \right)^2 \right\rangle \quad . \quad (3)$$

Again, for weak scintillation this is equivalent to the variance of $\log(I_A/I_B)$, but the definition (3) is preferable. It has been shown that the differential index in two concentric annular apertures is almost independent of the propagation distance z for $z > \sqrt{\lambda D_A}$, where D_A is the diameter of the smallest aperture (Tokovinin 1998, 2002b, 2003). The differential index in such apertures in nothing else but

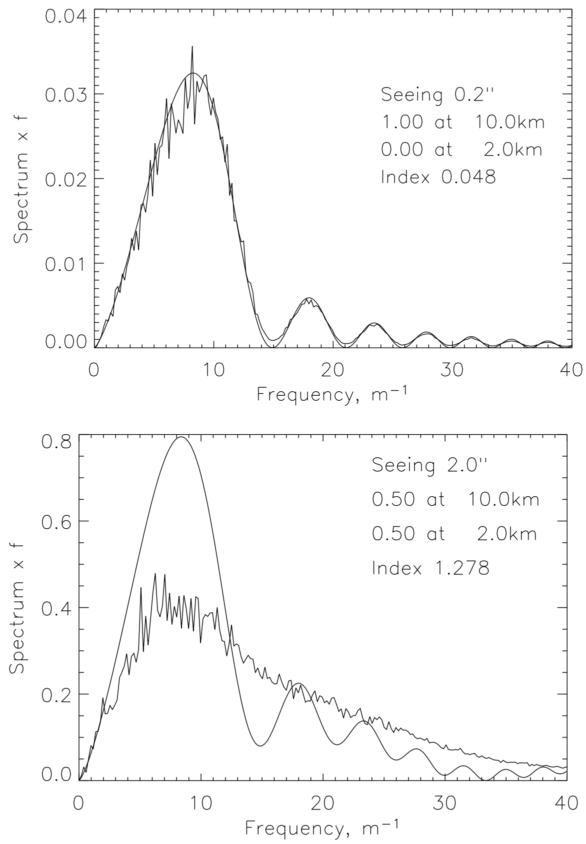

Fig. 2. Power spectra of scintillation produced at the ground. Smooth curves – analytical theory, Equation 1, "noisy" curves – direct numerical simulation. Top panel – weak turbulent layer at 10 km, bottom panel – strong scintillation when a $2''$ seeing is created by two equal layers at 2 km and 10 km.

the scintillation power filtered in the frequency band from $1/D_B$ to $1/D_A$. Thus, MASS with its centimetric apertures is sensitive to the turbulence of centimetric scales.

In the framework of the small-perturbation theory, both normal and differential scintillation indices s_k^2 depend on the turbulence profile $C_n^2\ (z)$ linearly as

$$s_k^2 = \int W_k(z)\ C_n^2\ (z) \mathrm{d}z \quad , \tag{4}$$

where the *weighting function* (WF), $W_k(z)$, describes the altitude response of a given aperture or aperture combination k (Tokovinin 2002b, 2003). If the WF is constant, it means that the scintillation index gives a direct measure of the turbulence integral, hence seeing. The differential index has this attractive property and thus provides a more-or-less direct measure of the seeing in the free atmosphere. This idea was published by Tokovinin (1998) and first tested the same year at Mt. Maidanak with a *Double-Aperture Scintillation Sensor*, DASS (Kornilov & Tokovinin 2001).

For normal scintillation indices, $W(z)$ increases as $z^{5/6}$ for small apertures or as z^2 for large ones (Roddier 1981). Steep dependence of the scintillation strength on altitude was an obstacle for measuring seeing by this method because we could not distinguish weak and high turbulence from the low and strong one. Differential indices have solved this problem.

The above formulae are valid only for weak scintillation, $s \ll 1$. This is so-called single-scattering, or Rytov approximation. In reality, the scintillation is not always weak, even at zenith. In this case, the spatial structure of the intensity fluctuations deviates from (1), sometimes quite significantly (Figure 2, bottom panel). Qualitatively, the deviation can be understood as a strong focusing, when turbulent "lenses" can produce bright, small spots at the ground. The size of such spots is smaller than the size of the lenses, so the power migrates to high frequencies. Alternatively, the effect can be seen as an appearance of second harmonics or combination frequencies in the intensity pattern created by strong phase gratings. Under strong scintillation, the combined effect of several layers is no longer additive, as predicted by Equation 4: high layers cross-modulate the scintillation produced by lower layers. There is no theory describing these effects in a quantitative manner, despite many years of theoretical work on strong scintillation (e.g., Andrews et al. 1999). Note that the low-frequency part of the spatial spectrum is not affected by saturation, so large-scale intensity fluctuations are still a simple consequence of the wave-front curvature, as prescribed by the geometrical optics.

Considering the scintillation of an extended source, say a disk of angular diameter θ, we must additionally multiply the spectrum (1) by a filter corresponding to a circle of diameter θz. At low altitudes where $\theta z < \sqrt{\lambda z}$ this additional filter has little effect, but at higher altitudes it dominates, admitting only low spatial frequencies. As a result, the scintillation is weakened, being produced only by large lenses. This is the regime where geometric optics is applicable, so such scintillation is achromatic (Kaiser 2004).

3. THE MASS INSTRUMENT

In the *Multi-Aperture Scintillation Sensor* (MASS) turbulence profiler (Kornilov et al. 2003), the light of a single bright star is detected by four concentric apertures which act as a spatial filter

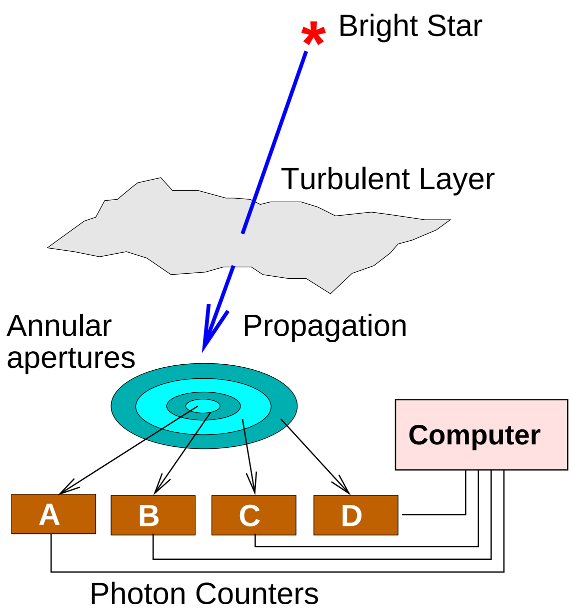

Fig. 3. Principle of the Multi-Aperture Scintillation Sensor, MASS.

(Figure 3). Photon counts in each aperture registered with an exposure time of 1 ms are processed to calculate 4 normal and 6 differential scintillation indices. These indices are then fitted to a model of 6 turbulent layers (Tokovinin et al. 2003) using Equation 4.

Most MASS instruments built to date are combined with a *Differential Image Motion Monitor*, DIMM (Sarazin & Roddier 1990) in a single device (Figure 4). It is attached to a small telescopes of 25-cm diameter or larger and shares the pupil between MASS and DIMM channels. The image of the exit pupil is formed by a lens inside the instrument on the *pupil plate*, where two DIMM mirrors and 4 concentric annular mirrors of MASS, *segmentator*, are located. The segmentator sends 4 beams A, B, C, and D to light detectors – miniature photomultipliers R74000 from Hamamatsu. The detectors and their photon-counting circuits are assembled in a very compact module which can be detached and replaced if necessary. The diameter of the outer MASS aperture (in projection on the entrance pupil) is about 8 cm, its inner aperture is about 2 cm.

An essential part of the MASS is its software, *Turbina*. Individual photon counts are not saved on the disk (although this can be done for technical purpose), but rather processed in real time to compute scintillation indices every second. After each minute, the average indices are calculated and the turbulence parameters are determined. The raw data (indices)

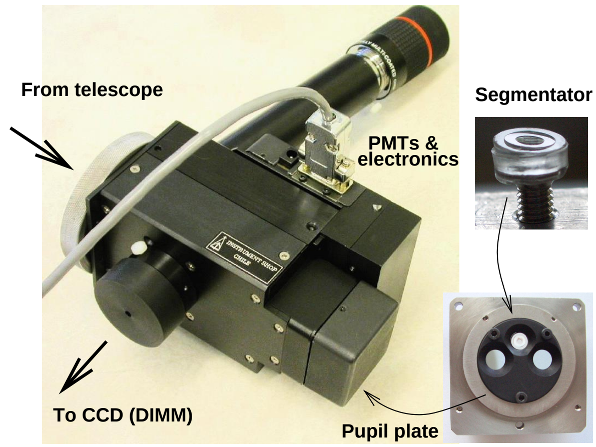

Fig. 4. MASS-DIMM instrument and main elements of its MASS channel.

and turbulence profiles are saved in the text files together with accompanying information which permits various sanity checks of the data.

4. ACCURACY OF MASS

MASS is essentially a fast photometer. However, its useful signal is not the flux, but rather its fluctuations, scintillation indices. Of course, even a constant light will produce fluctuating photon counts because of the shot noise, but this *bias* is subtracted in the data processing. Useful, atmospheric fluctuations are measured from $T = 1\,\mathrm{min}$. integrations. The relative error of the indices is determined by the statistics of the signal and is on the order of $(T/\tau)^{-1/2}$, where τ is the characteristic time of signal fluctuations. In practice, this error is about 2–3%, independently of the strength of scintillation. Thus, the relative random errors of MASS are essentially constant, except situations when the shot noise dominates (very weak turbulence and faint stars, especially for the s_{AB} index). In the restoration process, these errors translate to a random error of turbulence in each layer reaching 10% of the total integral (Tokovinin et al. 2003). Hence, turbulence strength of less than $10^{-15}\,\mathrm{m}^{1/3}$ in the MASS data files should be treated as zero.

The absolute calibration of MASS relies on the knowledge of the aperture geometry and spectral response – these quantities define the weighting functions and are used to translate measured scintillation indices into turbulence profiles. Practice and simulation show that the magnification factor defining the diameters of projected apertures must be measured to an accuracy of $\sim 3\%$. Needless to say that no change of the aperture geometry (e.g. by vignetting

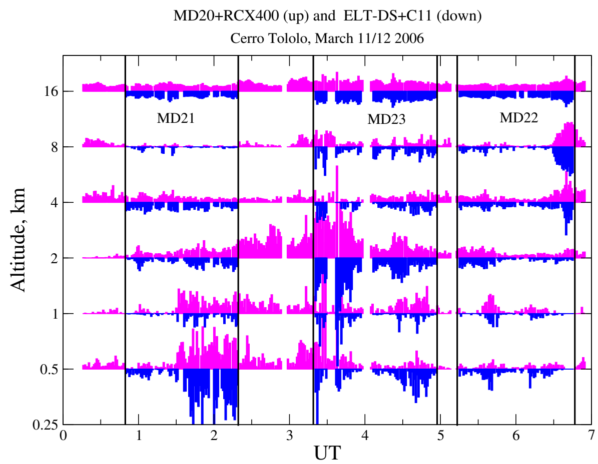

Fig. 5. Inter-comparison of MASS instruments (March 2006, Cerro Tololo). The length of the bars is proportional to the $C_n^2 \mathrm{d}h$ integrals in each layer and plotted against time. One MASS instrument was working continuously as a reference (upper bars), while three other instruments were use sequentially on a different telescope (lower bars).

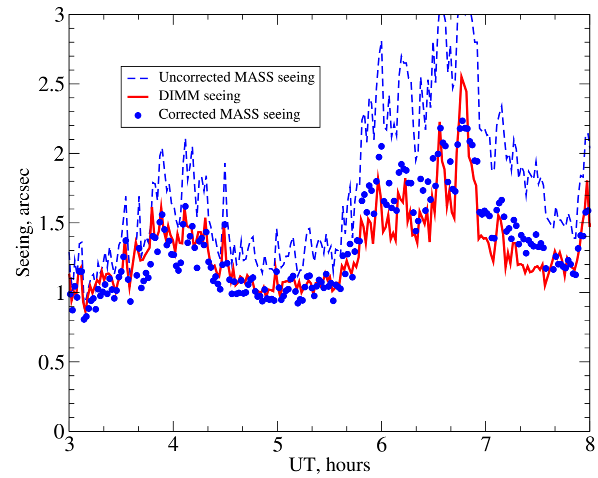

Fig. 6. "Over-shoots" of MASS and their correction. The data were taken at Cerro Tololo on October 7/8, 2004 when the seeing was dominated by high layers.

or non-uniform dust) is allowed. The spectral response is determined from the known properties of the detectors and optics and is checked by comparing the fluxes of stars of different colors with their expected fluxes. Of course, the color of the star itself influences the overall spectral response and is taken into account in the MASS software.

Despite careful calibration, all MASS instruments are slightly different, e.g. because of their individual detector characteristics. Comparison between two MASSes reveals that the integral parameters such as free-atmosphere seeing or isoplanatic angle usually match within few percent. The turbulence profiles are also similar, but their details may differ, sometimes in a systematic way (e.g. Figure 5). For example, one instrument may "think" that most of the turbulence is at 2 km, while another measures the same turbulence distributed between 1 km and 2 km. The agreement between instruments is always better for the two highest layers (8 km and 16 km) than for the lowest layers, because the scintillation from high altitudes is stronger. A direct comparison between MASS and Scidar (Tokovinin et al. 2005) leads to the same conclusion.

The free-atmosphere seeing measured by MASS should always be better or equal to the full seeing measured by DIMM. However, it was found that under strong turbulence, MASS typically measures a worse seeing, "over-shoots" (Figure 6). At first, this seemed counter-intuitive, as we expected that strong, saturated scintillation would under-estimate the turbulence strength. Numerical simulations (Figure 2) revealed that in fact under strong scintillation the power at high frequencies increases (compared to the weak-perturbation theory) and it is wrongly interpreted by the MASS software as scintillation produced by low layers. The turbulence profile is hence distorted (shifted to lower altitudes) and the seeing is over-estimated.

In the absence of strong-scintillation theory, the problem was tackled by numerical simulation. It was found that "over-shoots" can be approximately corrected if the turbulence integral measured by MASS is divided by $(1 + s_A)$. Further study led to a more elaborate scheme where all measured indices are corrected and then used in the standard profile restoration procedure (Tokovinin & Kornilov 2007). This method works for moderately strong scintillation, $s_A < 0.7$. Beyond this point, MASS does not give quantitative results, all we can say is that the turbulence in the upper atmosphere is very strong.

5. PLANET SCINTILLATION

The smallest MASS aperture is 2 cm, of the order of the Fresnel radius $\sqrt{\lambda h}$ for $h = 0.5$ km layer. Can we push this method to lower altitudes by using a smaller aperture, say 1 cm? In principle, yes, but we will need stars $\sim$20 times brighter. Not only the flux will be less, but the scintillation from low altitudes is weak, too. It would be difficult to separate this weak scintillation from the much stronger signal originating at high altitudes.

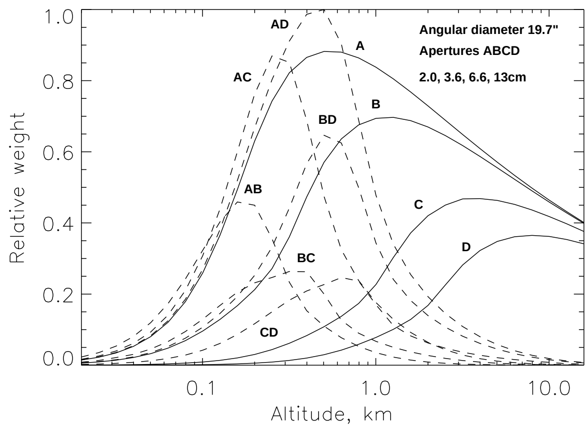

Fig. 7. Weighting functions for the scintillation of Saturn. Apertures and their combinations are marked by single and double letters for the normal and differential indices, respectively.

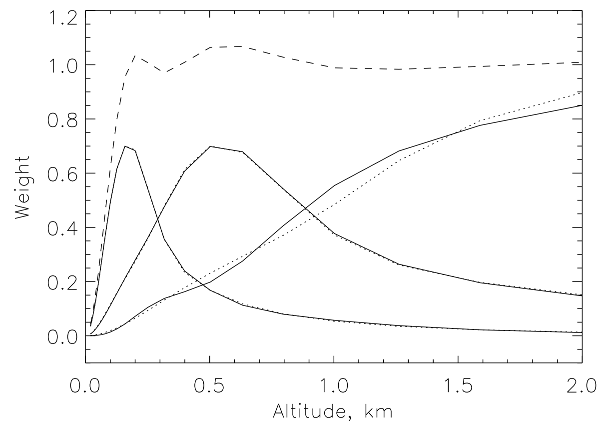

Fig. 8. Response of a planetary scintillometer corresponding to some linear combinations of the WFs. Full lines show the synthetic response for three layers – low, middle, and high. The dashed line is the sum of these response functions.

Planets are extended sources and scintillate much less because the signal from high-altitude layers is spatially averaged. As a result, the weighting functions for the normal indices decline at high altitudes, instead of growing (Figure 7), and the WFs for differential indices fall down rapidly. Thus, planetary scintillation "senses" turbulence located mostly in the first kilometer above ground. Interestingly, the condition $\max(D, \theta z) > \sqrt{\lambda z}$ is always fulfilled, so the scintillation signal is always averaged by either aperture (at low altitudes) or by the planet (at high altitudes) at spatial scales longer than the Fresnel radius. Therefore, planetary scintillation is described by the geometric optics and is achromatic.

The maxima of the WFs occur when those two averaging factors are comparable, i.e. at propagation distance $z \sim D/\theta$. If we want to probe a large zone of altitudes, a correspondingly large span of aperture sizes is needed. Depending on the angular diameter θ of the planet available on the sky, the sensitivity zone of a *planetary scintillometer* (PlaSci) moves closer or further away from the telescope. Moreover, the sensitivity is a function of the *range* $z = h/\cos\gamma$ instead of altitude h, i.e. it depends on the zenith distance γ. In a MASS, a star sufficiently close to the zenith can always be selected, so its results are related to the altitudes h. In contrast, the parameters of PlaSci depend on the available planet and change during the night as the planet moves on the sky.

Experiments with PlaSci were conducted at Cerro Tololo Inter-American Observatory (CTIO) on 4 nights in November-December 2004, when a Slodar turbulence profiler was tested and compared to Sodar. The data from Slodar, Sodar and MASS-DIMM provide a benchmark for evaluating the new method, PlaSci. The only planet available on the sky in this period was Saturn, visible in the morning at high air mass. In the data processing, we neglected the rings which contributed only few percent of the light, and calculated WFs for a uniform disk of angular diameter $19.7''$. A first-generation MASS instrument with apertures from 2 cm to 13 cm was used, with a neutral-density filter in the D-channel to prevent saturation of the photon counts.

Some WFs displayed in Figure 7 have maxima in the first kilometer and provide a measure of turbulence strength in this zone. A better job of turbulence profile restoration can be done by combining linearly the WFs with suitable coefficients. We used only three indices s_{AB}, s_{BD}, and s_C and found their linear combinations that better isolate three pre-selected layers (Figure 8). At air mass of $\sim$2, the first layers corresponded to altitudes of $\sim$100 m and $\sim$200 m above the observatory.

A comparison with MASS-DIMM have shown that PlaSci gives reasonable results, although the difference in the response functions of these instruments prevents a quantitative conclusion. In Figure 9, the seeing in the two PlaSci "layers" is compared to the seeing inferred from the acoustic sounder, Sodar, by integrating its profiles with the same response. Again, we see a qualitative agreement, but some quantitative differences. Note that at that time the

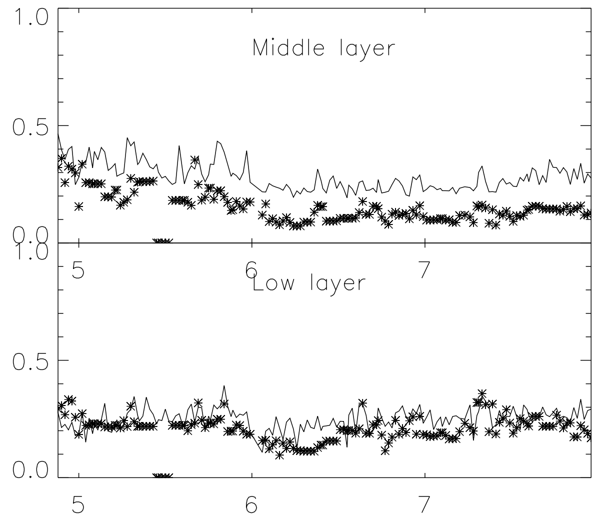

Fig. 9. Comparison between the low-altitude seeing (in arcseconds) measured with PlaSci (lines) and Sodar (asterisks) on December 1/2, 2004, at Cerro Tololo (horizontal axis – universal time). The low and middle layers are at altitudes of ∼100 m and ∼200 m, respectively

absolute calibration of Sodar was still uncertain, but it has improved since (Travouillon 2006).

Planetary scintillometer fulfills the promise to extend the MASS method to lower altitudes. However, the gain in the lower limit is only a factor of 2–4, not enough for a detailed characterization of the ground layer. The performance of the PlaSci method depends on the visibility of a suitable planet and its elevation. Hence, development of a regular turbulence monitor based on this idea appears problematic.

6. LUNAR SCINTILLOMETER

Sun with its angular diameter $\theta \approx 30'$ also scintillates. However, this scintillation has very low amplitude $s \sim 10^{-8}$ and originates mostly in the immediate vicinity of the instrument, at distances of few meters. Beckers (2001) proposed to use solar scintillation for turbulence profiling in the ground layer and developed the instrument, Shabar. It consists of 6 light detectors in a linear non-redundant configuration, with baselines up to 47 cm. Covariances between light fluctuations in individual detectors are measured and serve to restore the profile from ∼1 m to ∼100 m from the instrument. Shabars were used in combination with a solar DIMM to select the site for a new solar telescope (Socas-Navarro et al. 2005).

A Shabar using Moon as a light source can be built for night-time measurements. Compared to the Sun, there are however three additional challenges:

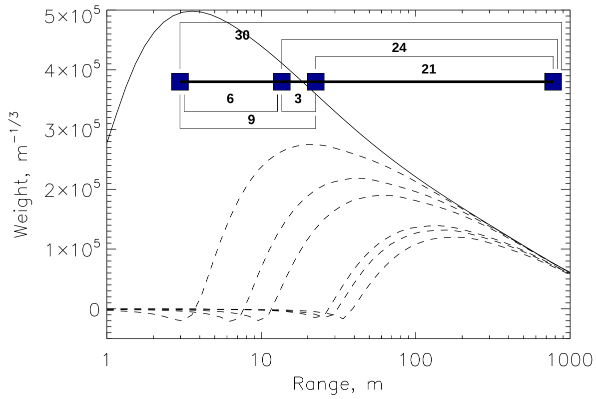

Fig. 10. The weighting functions $W(z, b)$ for the detector configuration 6-9-30 (baselines 0, 3, 6, 9, 21, 24, and 30 cm). The full line shows autocorrelation, dashed lines – cross-correlations. Full Moon, 1-cm detector, turbulence outer scale $L_0 = 25$ m.

- Moon's phases and surface detail
- Detectability of a small scintillation signal
- Methods of profile restoration

Hickson & Lanzetta (2004) prototyped lunar Shabar and made first measurements. Later, this group constructed a 12-channel lunar scintillometer and installed it at CTIO.[2] We also decided to develop a *lunar scintillometer*, LuSci. The idea was to address the above three challenges and to find the simplest possible instrument concept. Our primary motivation was to use such a scintillometer in Antarctica for detailed measurements of its highly-turbulent ground layer.

If the ground layer is blown in front of the detector by a steady wind, the temporal correlation function of the scintillation signal can be used instead of its spatial correlation. However, the wind speed profile $V(h)$ must be known, which is not usually the case. At each altitude h, the typical size of "lenses" contributing most of scintillation is θh and corresponds to the time delay $t = \theta h / V(h)$. If $V(h) =$ const., there is a unique mapping between t and h. In the worst case when $V(h) \propto h$ all layers produce temporal correlations of same width and cannot be disentangled. The idea of LuSci is to take advantage of the temporal correlations and to combine them with spatial correlations on few baselines. Presently we use only 4 detectors.

Figure 10 shows the WFs corresponding to the correlations of the scintillation signal on several baselines from 3 cm to 30 cm. The detector size is 1 cm

[2] See http://www.astro.ubc.ca/LMT/alpaca/site.html

square. Note that Hickson & Lanzetta (2004) used a simplified, non-rigorous expression for calculating the WFs, following Beckers (2001). These authors also ignored the finite turbulence outer scale. In fact the averaging size θz reaches 10 m at $z > 1$ km, and the deviation of turbulence spectrum from the Kolmogorov model becomes very significant, reducing the scintillation. Socas-Navarro et al. (2005) discovered this circumstance empirically and had to account for it by introducing an extra parameter, "missing scintillation".

The first challenge – Moon's phases – was addressed by calculating the scintillation covariance with actual Moon images. It turns out that for the period of ± 5 days around full Moon the model of an elliptical disk reproduces the actual scintillation covariances with an absolute error of 10% of the variance or less. The largest error at zero baseline (variance) is caused by the neglect of surface details in the elliptical disk model. Covariances at non-zero baselines are modeled even more accurately, being less sensitive to fine details.

The detector for measuring lunar scintillation must reliably register relative flux fluctuations of 10^{-5} at frequencies of few hundred Hz. A 1-cm Si photo-diode gives a photo-current of 90 nA (or $5.5\ 10^{11}$ photo-electrons s^{-1}) from the full Moon. The shot noise of this signal in 1-ms integration time corresponds to relative fluctuations $\Delta I/I \sim 4 \times 10^{-5}$. It turns out that the noise of common operational amplifiers (e.g. LT 1464) is much less, so our detector is nearly perfect. Of course, care is taken to avoid any pick-up noise (grounding, shielding, etc.). The dynamic range of 16-bit converters is insufficient for digitizing small signal fluctuations, hence we amplify the fluctuating part by 100 times and digitize it separately from the DC part, as done by Hickson & Lanzetta (2004).

The last challenge – profile restoration – is approached by the same method as used for planets, i.e. by finding linear combinations of covariances that peak at certain altitudes and are close to zero elsewhere. It is clear that the WFs have sharp cutoffs at $z < \theta b$, where b is the baseline (Figure 10). Even a simple difference of two WFs at baselines b_1 and b_2 will isolate a range $b_1/\theta < z < b_2/\theta$. Our method of finding suitable linear combinations is more elaborate than a simple difference, but essentially similar. Response functions obtained by this technique are plotted in Figure 11. The half-width of the response $\Delta z/z \sim 1$ defines the altitude resolution. With a larger number of detectors and baselines, a higher resolution will be possible.

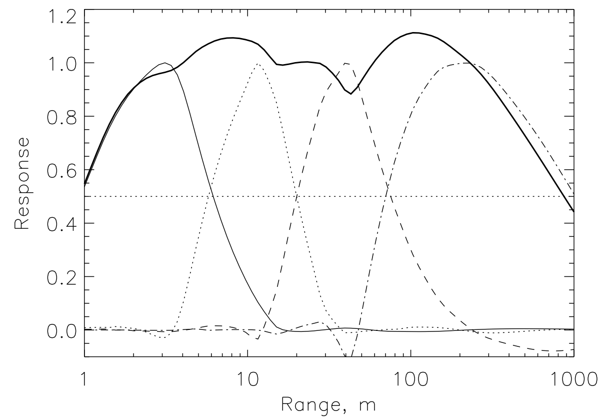

Fig. 11. Response functions of LuSci for baseline configuration 3-10-38 and layers centered at 3, 12, 40, and 200 m. The thick line shows a sum of responses.

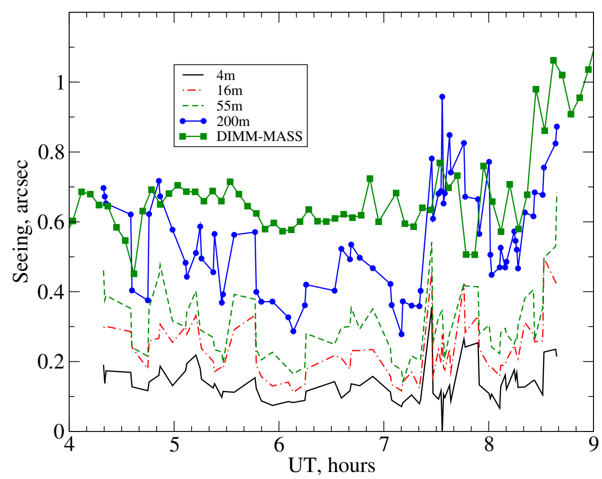

Fig. 12. Ground-layer seeing measured by LuSci and estimated by the DIMM-MASS on February 5/6, 2007 at CTIO. The curves for LuSci depict seeing created by turbulence from the ground up to the indicated altitude.

The grid of "layers" is defined above as a function of range, not altitude, so it projects to altitudes with a $\cos\gamma$ compression depending on the Moon's zenith distance γ. The distance of the peak response cannot be selected arbitrary, as it related to the cutoffs of the WFs. Hence, it is not possible to re-define response in terms of altitude $h = z \cos\gamma$, as in MASS.

Figure 12 shows how this restoration technique works on the real data. The ground-layer seeing was calculated by taking the first LuSci layer, sum of the first two layers, etc. No correction for the air mass was applied because the thickness of the layers is proportional to $\cos\gamma$ and thus compensates for the air-mass effect for a uniform $C_n^2(h)$ profile. The seeing in the ground layer (GL) up to ~500 m was measured simultaneously by subtracting turbulence integrals delivered by DIMM and MASS (with 5-min. averaging). The results of LuSci show that on that particular night, the ground-layer seeing was not dominated by turbulence in the first ~20 m, as one would expect, but was rather produced by the whole 500-m zone. Apparently, the LuSci's upper sensitivity limit was lower than 500 m, so sometimes it measured the GL seeing less than the DIMM-MASS. Both instruments show correlated details in the temporal variation of the GL seeing.

The temporal auto- and cross-correlations of the lunar scintillation signal at two baselines are shown in Figure 13. The narrow peak is produced by small-scale structures at low altitudes. In the covariance on a 10-cm baseline this peak is displaced from the coordinate origin by ~0.1 s, corresponding to a projected wind of $V \sim 1\,\mathrm{m\ s}^{-1}$ along the baseline (the wind on February 5/6 was weak). This narrow peak is absent in the covariance at the longest 38-cm baseline because the wind vector was not oriented along the baseline. The slow component of the signal corresponds to a turbulence at few hundred meters, it is correlated on all baselines. This example shows that temporal analysis of the scintillation signal adds significant information to the spatial covariances. We plan to further develop this approach.

LuSci is a relatively simple and robust method for quantitative measurement of turbulence profile near the ground. The scintillation signal, although weak, can be detected reliably. The theory of lunar scintillation is very simple (geometrical optics, no saturation) and the Kolmogorov model is adequate in the range of measured spatial scales (from few cm to 1 m). The resolution of a simple 4-channel instrument is already adequate for determining the height of a telescope dome (see Socas-Navarro et al. 2005, for an example of data use) and can be further improved by adding additional detectors or, better, by using the temporal domain. LuSci is cheaper and more accurate than the micro-thermal mast equipment traditionally used for GL turbulence studies.

7. WHAT'S NEXT?

The theory of optical propagation through turbulence was established over 50 years ago. Yet, an explosive development of new techniques for optical turbulence measurements happened only recently, in the past few years. A stimulus for such development was provided by the needs of adaptive optics and interferometry, but an even more important factor is the progress of technology. Without modern detectors and computers, instruments like MASS and LuSci would not be practical, although in principle they could be envisioned long time ago.

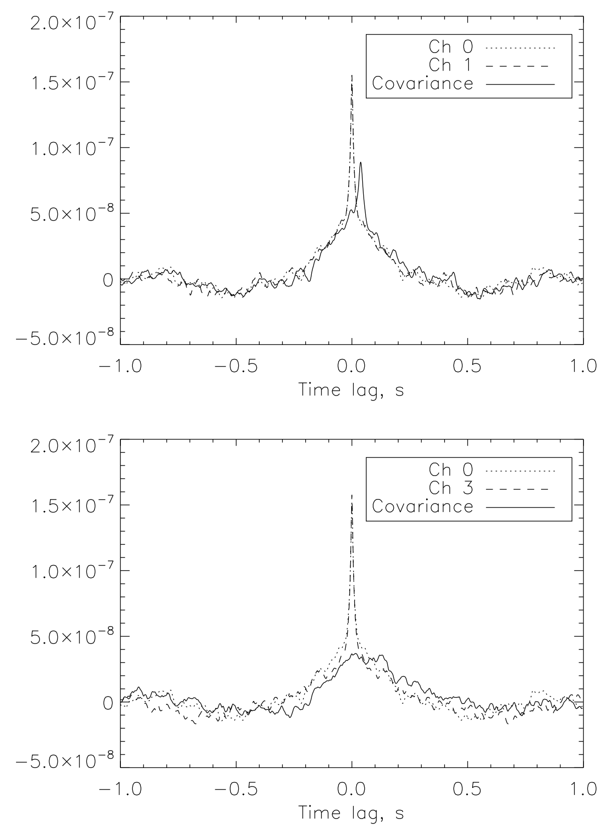

Fig. 13. Temporal covariances of Moon's scintillation with baselines 10 cm (top) and 38 cm (bottom). Data taken on February 5/6, 2007, at 7:45 UT.

As new, better and cheaper detectors become available, new ideas on how to use them for turbulence characterization will emerge. Instead of the 4 channels of MASS, a complete 2-dimensional analysis of the scintillation pattern will become feasible, as already implemented in the single-star scidar (Habib et al. 2006). The methods of data interpretation will evolve, too.

There is little doubt that the need to monitor turbulence profiles near the ground and in the whole atmosphere will not vanish – on the contrary, almost every observatory will eventually want to have a new, advanced site monitor. Among many existing and future instruments, the users will prefer the simplest and cheapest options with automatic on-line data processing and robotic control. The MASS-DIMM instrument comes close to this ideal, but it is not the last word. The development will continue!

REFERENCES

Andrews, I. C., Phillips, R. L., Hopen, C. Y., & Al-Hanash, M. A. 1999, J. Opt. Soc. Am. A, 16, 1417

Beckers, J. 2001, Exp. Astron., 12, 1

Fuchs, A., Tallon, M., & Vernin, J. 1998, PASP, 110, 86

Habib, A., Vernin, J., Benkhaldoun, Z., & Lanteri, H. 2006, MNRAS, 368, 1456

Hickson, P., & Lanzetta, K. 2004, PASP, 116, 1143

Kaiser, N. 2004, Site Evaluation using Lunar Shabar, Pan-STARRS internal memo `http://pan-starrs.ifa.hawaii.edu/project/events/talks/2004_01_23_kaiser.pdf`

Kenyon, S., Lawrence, J. S., Ashley, M. C. B., Storey, J. W. V., Tokovinin, A., & Fossat, E. 2006, PASP, 118, 924

Kornilov, V. G., & Tokovinin, A. A. 2001, Astron. Rep., 45, 395

Kornilov, V., Tokovinin, A., Voziakova, O., Zaitsev, A., Shatsky, N., Potanin, S., & Sarazin, M. 2003, Proc. SPIE, 4839, 837

Krause-Polstorf, J., Murphy, E. A., & Walters, D. L. 1993, Appl. Opt., 32, 4051

Ochs, G. R., Wang, T.-I., Lawrence, R. S., & Clifford, S. F. 1976, Appl. Opt., 15, 2504

Roddier, F. 1981, Prog. Optics, 19, 281

Sarazin, M., & Roddier, F. 1990, A&A, 227, 294

Socas-Navarro, H., et al. 2005, PASP, 117, 1296

Tatarskii, V. I. 1961, Wave propagation in a Turbulent Medium (New York: Dover)

Tokovinin, A. A. 1998, Astron. Lett., 24, 662

———. 2002a, PASP, 114, 1156

———. 2002b, Appl. Opt., 41, 957

———. 2003, J. Opt. Soc. Am. A, 20, 686

Tokovinin, A., Kornilov, V., Shatsky, N., & Voziakova, O. 2003, MNRAS, 343, 891

Tokovinin, A., Vernin, J., Ziad, A. & Chun, M. 2005, PASP, 117, 395

Tokovinin, A. & Kornilov, V. 2007, MNRAS, accepted (arXiv:0708.0195v1)

Travouillon, T. 2006, Proc. SPIE, 6267, 626720